Genomic insights into population dynamics and adaptive strategies of the endangered dipterocarp, Hopea chinensis

By Xiang, W., Jiang, Y., Zou, J., Deng, Y., Jiang, K., Zhang, K., Zhou, X., Quan, K., Han, Z., Liu, W., Tang, L., Li, Y., Segar, S.T., Zhang, Y., Hu, X., Wang, R. and Chen, X.

Harper Adams University

Original research article

Genomic insights into population dynamics and adaptive strategies of the endangered dipterocarp, *Hopea chinensis*

Wei-Min Xiang [a,1], Yu-Ting Jiang [a,1], Jie Zou [a,1], Yan Deng [a], Kai Jiang [b], Kai-Jian Zhang [c], Xin-Yu Zhou [a], Kai-Xi Quan [a], Zi-Wen Han [a], Wei-Chao Liu [a], Liang Tang [d], Yuan-Yuan Li [a], Simon T. Segar [e], Yuan-Ye Zhang [f], Xing-Hua Hu [g,*], Rong Wang [a,h,i,**], Xiao-Yong Chen [a]

[a] *Zhejiang Tiantong Forest Ecosystem National Observation and Research Station, Shanghai Key Lab for Urban Ecological Processes and Eco-Restoration, School of Ecological and Environmental Sciences, East China Normal University, Shanghai, China*
[b] *Shanghai Key Laboratory of Plant Functional Genomics and Resources, Shanghai Chenshan Botanical Garden, Shanghai, China*
[c] *Novogene Bioinformatics Institute, Beijing, China*
[d] *Key Laboratory of Genetics and Germplasm Innovation of Tropical Special Forest Trees and Ornamental Plants (Hainan University), Ministry of Education, Haikou 570228, China*
[e] *Agriculture & Environment Department, Harper Adams University, Newport, United Kingdom*
[f] *Key Laboratory of the Ministry of Education for Coastal and Wetland Ecosystems, College of the Environment and Ecology, Xiamen University, Xiamen, Fujian Province, China*
[g] *Guangxi Institute of Botany, Guangxi Zhuang Autonomous Region and the Chinese Academy of Sciences, Guilin 541006, China*
[h] *Shanghai Engineering Research Center of Sustainable Plant Innovation, Shanghai, China*
[i] *Institute of Eco-Chongming, Shanghai, China*

ARTICLE INFO

ABSTRACT

Asian rainforests are a biodiversity hotspot and are dominated by dipterocarps. Thus, protecting endangered dipterocarp species living on the distribution boundary of dipterocarps is a central factor in maintaining the range of Asian rainforests. Despite the perceived conservation priority of these species, we know little about how they became endangered and how they have adapted to marginal habitats. Here, we focused on the population genomics of *Hopea chinensis*, an endangered species narrowly distributed at the northern limit of dipterocarps, to (1) reveal its demographic history and infer factors contributing to endangered status; (2) evaluate the genetic consequences of its small remnant population; and (3) identify key genes associated with its adaptation. We found drastic population declines after the Last Glacial Maximum, suggesting the role of human disturbances in the endangered status. Despite high levels of inbreeding, we detected only 441 derived deleterious and 337 derived major-effect mutations, which were not significantly enriched in any KEGG pathway, providing evidence of low genetic loads. Furthermore, selective sweep analysis showed 12 genes associated with cold and drought tolerance and plant defense and immunity. Comparative genomics identified 125 specific and 30 lost gene families in the genome of *H. chinensis*, many of which were relevant to the responses to biotic and abiotic stresses. Our findings, therefore, reveal the genomic characteristics linked with the endangered status and adaptations for *H. chinensis*. Together with the population genomic results

* Correspondence to: No. 85, Yanshan Road, Guilin 541006, China.
** Correspondence to: No. 500, Dongchuan Road, Minhang District, Shanghai 200241, China.
E-mail addresses: huxh773@163.com (X.-H. Hu), rwang@des.ecnu.edu.cn (R. Wang).
[1] These authors contributed equally: Wei-Min Xiang, Yu-Ting Jiang, and Jie Zou.
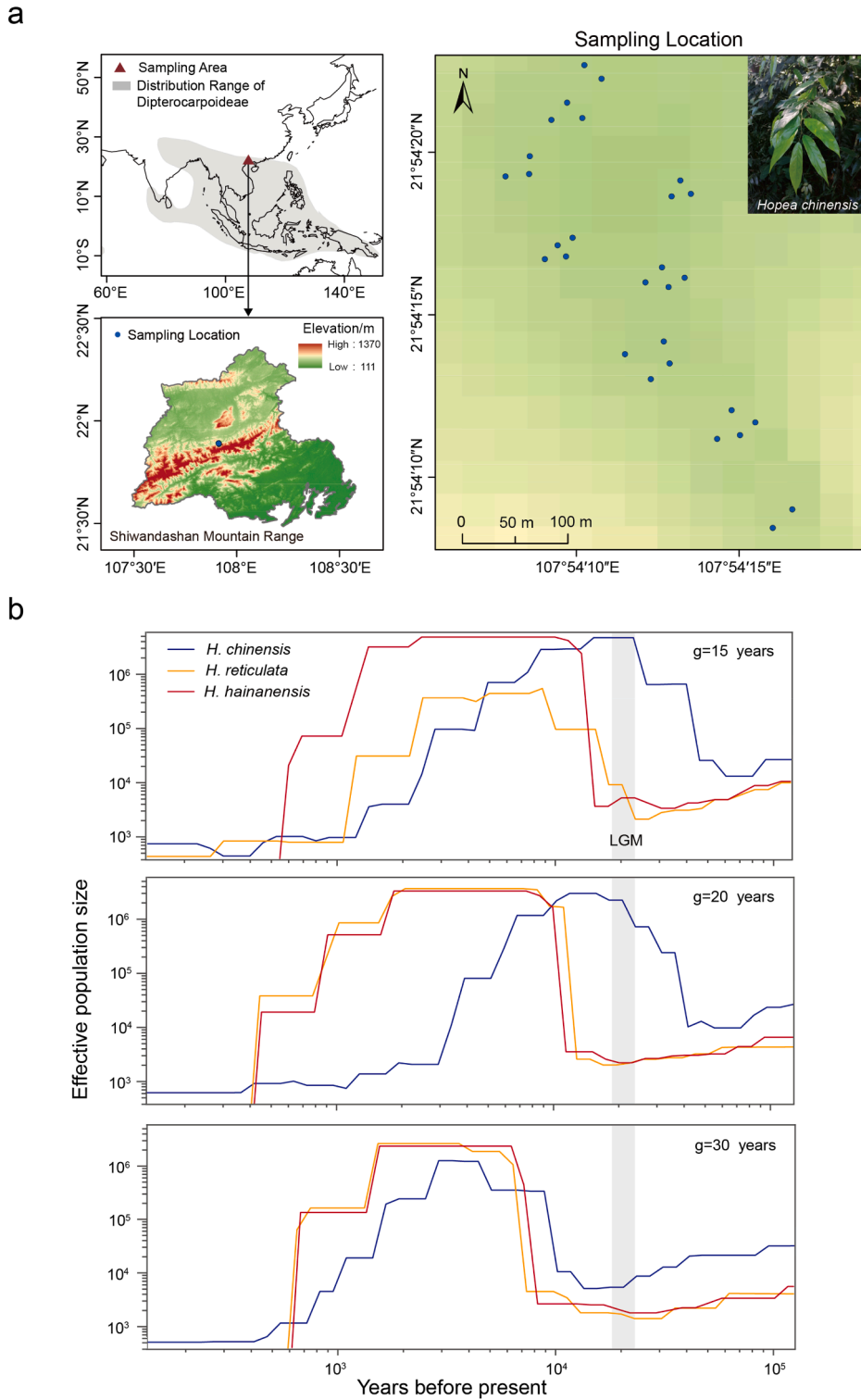
Fig. 1. Sampling locations of wild *H. chinensis* trees for population genomics **(a)**, and demographic history of *H. chinensis*, *H. hainanensis* and *H. reticulata* **(b)**. **(a)**, We determine the distribution range of Dipterocarpoideae based on the description of Ashton et al., (2021). **(b)**, Population dynamics of *H. chinensis* are analyzed using SMC++, and the Last Glacial Maximum (LGM) is highlighted in light grey. We illustrate the demographic history of *H. hainanensis* and *H. reticulata* according to the results of SMC++ in Wang et al., (2024).

from two other dipterocarp species, we highlighted the necessity to establish nature reserves to prevent further human disturbances and to comprehensively describe the mutualistic and antagonistic networks associated with endangered dipterocarp species to guide *in-situ* and *ex-situ* conservation.

1. Introduction

Asian rainforests are a biodiversity hotspot harboring exceptionally rich species and contributing crucially to the global ecosystem functioning (Myers et al., 2000; Wilcove et al., 2013). However, Asian rainforests are disappearing rapidly, and severe logging and land use changes have led to an annual reduction of *c.* 0.6 % of their total area (Stibig et al., 2014; Wilcove et al., 2013). The range of this ecosystem is dominated by dipterocarps, species in the subfamily Dipterocarpoideae (Dipterocarpaceae) (Raes et al., 2014). Dipterocarps are typically found in Southeast Asia, India, and Seychelles (Fig. 1a), and are famous for giant adults accounting for almost all emergent and over 50 % canopy trees in Asian rainforests (Bansal et al., 2022; Ghazoul, 2016). Despite the high species richness (about 470 species) of this subfamily, 75 % of all dipterocarp species are endangered (https://www.iucnredlist.org/). Therefore, effectively conserving endangered dipterocarps is essential for protecting and restoring Asian rainforests (Ashton and Kettle, 2012; Ashton et al., 2021).

A prerequisite for designing appropriate strategies for both *in-situ* and *ex-situ* conservation is to identify the factors causing the endangered species' endangerment and explore how they adapt to their natural habitats (Li et al., 2021; Ma et al., 2021). Genomic and phylogenetic studies have found a Western Gondwanaland/Africa origin of dipterocarps and have established a likely migration route from Africa to India in the late Cretaceous through Kohistan-Ladakh Island Arc and subsequently to Southeast Asia during the middle to late Eocene after India-Asia collision (Bansal et al., 2022; Wang et al., 2024). However, more recent demography has been revealed only in two dipterocarp species (Wang et al., 2024). There are currently no studies concerning adaptations at the population level. Therefore, besides the ongoing protection efforts mainly considering the human impacts on habitat quality and ecological processes (Li et al., 2023; Primananda et al., 2023), it is necessary to infer the historical events leading to population declines and to reveal the molecular signals evolved in response to stresses.

Foundation species distributed at the geographic boundary of an ecosystem can offer novel insights into the adaptive limits, contributing to predicting range shifts of the ecosystem under the ongoing global changes (Gould et al., 2014; Takahashi et al., 2016). The extinction of dipterocarp species living on the distribution edge of Dipterocarpoideae may even narrow the range of Asian rainforests, as this ecosystem is dominated by dipterocarps (Raes et al., 2014). Thus, protecting genetic resources against rapid climate and environmental changes and avoiding further range contraction of Asian rainforests mean prioritizing the conservation of these endangered dipterocarps.

Hopea chinensis (Merr.) Hand.-Mazz. is an endangered dipterocarp species (Barstow, 2021). This species is naturally distributed at the northern boundary of the dipterocarps' range and was reported only in some mountainous areas and islands in Yunnan and Guangxi (China) and Quang Ninh (Vietnam) (Jin et al., 2015; Trang and Triest, 2016). At present, detailed locations of its wild trees are only recorded in the nature reserve of Shiwandashan (Guangxi) (Tang et al., 2018, 2009). Like many other dipterocarps, this tree produces fragrant oleoresins and high-quality timber, and thus its endangered status may be the result of long-term overexploitation (Huang et al., 2008; Wang et al., 2022). Nevertheless, historical climate and environmental changes such as the Last Glacial Period (LGP) are also likely to drive the population decline of dipterocarps (Ghazoul, 2016; Wurster et al., 2010). Moreover, compared with more southerly distributed dipterocarps, *H. chinensis* is found in relatively cool and dry environments (Tan et al., 2005). While we can expect an accordingly distinct composition of pathogens and herbivores, how this species responds to biotic and abiotic environments remains unexplored. A recent publication of a high-quality genome of *H. chinensis* (Wang et al., 2024) enables population genomic studies, which can provide robust insights into its demography and adaptations.

In this study, to test the role of human activities in the endangered status of *H. chinensis* and if local biotic and abiotic stresses had left significant footprints in its genome, we sampled its wild trees in the nature reserve of Shiwandashan and conducted population genomics and comparative genomics. We aim to (1) reveal the demographic history of *H. chinensis* and infer factors contributing to its endangered status; (2) evaluate the genetic consequences of its small remnant population size; and (3) identify key genes associated with its adaptation to the northern boundary of Dipterocarpoideae.

2. Methods

2.1. Sample collection and sequencing

Hopea chinensis is a narrowly distributed and endangered dipterocarp species, with the precise locations of its wild individuals only recorded in the nature reserve of Shiwandashan, Guangxi, China (Huang et al., 2008). To conduct population genomics, we collected fresh young leaves from 29 identified wild trees with a minimum interval of 25 m in September 2022 (Fig. 1a). Collected leaf materials were sterilized using 75 % alcohol, quickly dried using silica gel, and stored at –80 ℃.

For each sampled tree, we extracted total genomic DNA from leaf tissues using DNAsecure Plant Kits (TIANGEN), and genomic DNA libraries were constructed and sequenced using the Illumina HiSeqX platform (an insert size of 350 bp), generating 150 bp paired-end reads. For quality control, total raw data were filtered to obtain clean data using fastp ver.0.19.7 (Chen et al., 2018), and the raw

paired-end reads were trimmed according to the following conditions: (1) reads with adapter; (2) reads with $\geq$ 10 % unidentified nucleotides or $\geq$ 50 % bases having a quality score $\leq$ 5 in a single-end sequenced read.

2.2. Alignment and SNP calling

To accurately identify single nucleotide polymorphism loci (SNPs), the clean data were aligned to the latest published reference genome of *H. chinensis* (PRJNA1056647) (Wang et al., 2024), and we generated BAM files using BWA-MEM (Li and Durbin, 2009) based on the parameter settings: mem -t 4 -k 32 -M. Duplicated reads in the alignment results were removed using SAMTOOLS ver.1.3 (Li et al., 2009) with the command 'rmdup'. BAM files were then input into GAKT ver.4.0.4.0 (McKenna et al., 2010) to detect single nucleotide variants (SNVs) using HaplotypeCaller with default parameters, according to the filtering conditions: OD < 2.0, QUAL < 30.0, SOR > 3.0, FS > 60.0, MQ < 40.0, MORankSum < -12.5 and ReadPosRankSum < -8.0. Based on SNVs, SNPs were identified using VCFtools following the standards of minimum depth $\geq$ 13, minor allele frequency (MAF) $\geq$ 0.05, and missing rate $\leq$ 0.2. The SNPs were annotated using ANNOVAR (Wang et al., 2010) according to the annotation in the reference genome, and SNPs were classified into intergenic and genic regions.

2.3. Population demography

To explore the demographic history of *H. chinensis*, the effective population size (N_e) of sampled trees at different stages was estimated using PSMC ver.0.6.4-r49 (Li and Durbin, 2011) and SMC++ ver.1.15.5 (Terhorst et al., 2017). Both estimations used the same generation times (g) (g = 15, 20, and 30 years) and mutation rate (μ). To ensure our results are comparable with those from other two *Hopea* species, we used the mutation rates (g = 15, μ = 1.06 $\times$ 10^{-8} per site per generation; g = 20, μ = 1.41 $\times$ 10^{-8} per site per generation; and g = 30, μ = 2.11 $\times$ 10^{-8} per site per generation) as Wang et al. (2024), which were the average μ values from the three pair-wise calculations among *H. chinensis, Hopea hainanensis,* and *H. reticulata*.

Because the accuracy of the PSMC is mainly restricted within the period of over 20 thousand years (kyr) to 3 million years (Myr) ago (Li and Durbin, 2011), we inferred the ancient variations of N_e using PSMC with parameter: psmc -N30 -t15 -r5 -p 4+25*2+4+6. To obtain the fastq files with whole-genome consensus sequences, BAM files were first mapped to reference genome using SAMTOOLS ver.1.6 for generating VCF files, which were switched to consensus sequences using bcftools and were transformed to fastq files using vcfutils.pl setting parameters: vcfutils.pl vcf2fq -d 10 -D 100 -Q 20.

To further explore the recent-past population dynamics of *H. chinensis*, we implemented demographic analysis using SMC++, which is considered to have high accuracy for estimation of N_e within 10 kyr (Terhorst et al., 2017). The SMC++ input files were converted from VCF files, including filtered SNPs, using the command 'vcf2smc' and the default parameter settings. To test if different dipterocarps experienced similar demographic histories, we compared our SMC++ results with those from *H. hainanensis* and *H. reticulata* (Wang et al., 2024).

2.4. Evaluation of inbreeding

To assess the inbreeding level in the *H. chinensis* population, the frequency distribution and total length of the runs of homozygosity (ROH) were estimated based on SNP data using PLINK ver.1.07 (Purcell et al., 2007), with a sliding window size of 20 SNPs. The valid length of ROHs was larger than 5 Kb, and a valid calculation must contain at least 10 SNPs. In addition, FROHs (the total length of ROH divided by genome size) were calculated and compared with the results from *H. hainanensis* and *H. reticulata* (Wang et al., 2024) to further evaluate the inbreeding level of *H. chinensis*.

2.5. Detection of derived deleterious mutations

To investigate genetic loads of *H. chinensis*, we identified the derived deleterious mutation (DDMs) and the derived major-effect mutations (DMEMs). Nonsynonymous SNPs were identified based on SNP data according to genome annotation, and deleterious mutations (DMs) were identified using PROVEAN ver.1.15 (Choi et al., 2012) and SIFT4G ver.2.0.0 (Ng and Henikoff, 2003), where a nonsynonymous mutation with a score < -2.5 in PROVEAN or < 0.05 in SIFT4G was considered deleterious. Moreover, the mutations influencing transcription and translation were identified as major-effect mutations (MEMs), which were identified manually with the help of annotation information. DDMs and DMEMs were determined according to derived alleles, which were identified from the comparison of genomes of *H. chinensis* and *H. hainanensis* with the outgroup *H. reticulata*, and that of *H. chinensis* and *H. reticulata* with the outgroup *H. hainanensis*. Only the DDMs supported by both analyses were used for the following analysis. Genes, including DDMs and DMEMs, were assigned to various KEGG pathways using enrichment analysis (Kanehisa and Goto, 2000). Homozygous DDMs and DMEMs in at least one sample were selected and compared with the results from *H. hainanensis* and *H. reticulata* (Wang et al., 2024).

2.6. Genetic structure

To uncover the genetic structure of *H. chinensis* and inform sweep selective analysis, we used three approaches, including genetic clustering, phylogenetic analysis, and principal component analysis (PCA). To decrease the effects of linkage disequilibrium (LD) in genetic clustering and PCA, we used PLINK to retain only the SNPs located in noncoding regions with LD coefficient (r^2) < 0.1. Genetic clustering was performed using ADMIXTURE ver.1.23 (Alexander et al., 2009) with *K* values from 1 to 8, and the *K* with the minimum

cross-validation error was chosen as the optimal. Bootstrapping (bootstrap = 200) was used to detect the standard errors of parameters when assigning the sampled trees to different genetic clusters. PCA was conducted using GCTA ver.1.24 (Yang et al., 2011), and the top two principal components were extracted for the assignment of our samples. Phylogenetic relationships among samples were estimated based on a neighbor-joining tree (treebest nj -b 1000) constructed using TreeBeST ver.1.9.2 (Vilella et al., 2009).

2.7. Selective sweep analysis

For the detection of positive selection signals in the genomes of our studied *H. chinensis* population, three different statistics, including composite likelihood rate (CLR) (Williamson et al., 2007), nucleotide diversity (π), and Tajima's *D* (Tajima, 1989) were calculated based on filtered SNPs. Tajima's *D* and π were calculated using VCFtools with a sliding windows size of 10 Kb and step size of 5 Kb. CLR was calculated using SweeD ver.3.2.1 (Pavlidis et al., 2013) with a sliding window size of 10 Kb. Sites located in regions with negative Tajima's *D*, lowest top 5 % π, and highest top 5 % CLR values were identified to have positive selection signals. To infer the relationship between genes with positive selection signals and adaptation, genes harboring sites with positive selection signals supported by all three statistical methods were enriched in the KEGG pathways. The roles of genes with positive selection signals in response to biotic/abiotic stress were inferred from the published works of literature.

2.8. In vitro functional validation of a positively selected gene

To verify whether the function of positively selected genes is consistent with the annotation, we chose the indole-3-pyruvate monooxygenase (YUCCA) that catalyzed indole-3-pyruvic acid (IPA) into indole-3-acetic acid (IAA) (Yamamoto et al., 2007). To obtain the recombinant protein, the *YUCCA* gene was synthesized and cloned into pSmart-I plasmids, then expressed in *E. coli* strains BL21(DE3). The purification of recombinant proteins (purity > 90 %) was tested using SDS-PAGE with modified nickel-nitrilotriacetic acid agarose (Thermo Fisher Scientific).

To test the enzyme activity, 200 μg purified recombinant protein was added into a reaction system (1 ml) composed of 1000 μM IPA, 400 μM flavin adenine dinucleotide disodium salt hydrate (FAD), 10 μM β-Nicotinamide adenine dinucleotide 2′-phosphate reduced tetrasodium salt (NADPH), and phosphate buffered saline (PBS) buffer (pH = 7.4). The reaction system was incubated for 5 min and reacted for 15 min. The products were centrifuged using Centrifuge 5424 R (Eppendorf, Germany) at 12,000 rpm after overnight storage at −20℃. The products were detected in a UPLC combined with a QTRAP® 6500 + MS system equipped with an electrospray ionization (ESI) source (AB SCIEX). Parameters were determined by infusion of IAA standard (100 ng/ml). The ESI parameters for negative mode were: ion spray voltage, 5500 V; heated probe temperature, 400 ℃ curtain Gas, 35 psi; cone temperature, 550 ℃; probe gas flow, 55 psi; nebulizing gas, 55 psi. The catalyzed IAA was separated from products using a Kinetex C18 column (2.6 μm, 2.1*100 mm, Phenomenex), and we used Analyst ver.1.6.3 (AB SCIEX) to analyze data. This enzyme activity assay was repeated three times, and controls were set without adding the enzyme.

2.9. Comparative genomics

For further exploring the species-specific molecular footprints of adaptations in the genome of *H. chinensis*, we compared the genome of *H. chinensis* with four genomes of other dipterocarp species (*Dipterocarpus turbinatus*: PRJNA1056647, *Parashorea chinensis*: PRJNA1056647, *Shorea robusta*: PRJNA1056647 and *Vatica mangachapoi*: PRJNA1056647). Gene families of these five dipterocarp species were clustered using OrthoMCL ver.2.0.9 (Li et al., 2003), with a criterion of $e < 1 \times 10^{-5}$ in 'all-versus-all' BlastP. The single-copy orthologs that experienced positive selection were detected by the branch-site model using PAML ver.4.9 (Yang, 2007). We characterized expanded and contracted gene families in the *H. chinensis* genome using CAFE ver.2.1 (De Bie et al., 2006), setting default parameters. Positively selected genes and genes in contracted/expanded families were enriched into KEGG pathways. Moreover, we manually identified the gene families that were only present (specific gene families) or completely absent (lost gene families) in the *H. chinensis* genome, and their potential contributions to the responses to biotic/abiotic stresses were determined through comparisons to the published works of literature.

3. Results

3.1. Genome resequencing

We collected leaf tissues from 29 wild trees of *H. chinensis* in the nature reserve of Shiwandashan, where the wild trees of this species are only distributed in an extremely narrow range (about 200 m × 400 m) (Fig. 1a). Using the Illumina platform, we obtained 482.9 Gb clean pair-end sequencing data from our sampled trees (Table S1). After mapping clean reads to the reference *H. chinensis* genome (Wang et al., 2024), we detected a high mapping ratio (mean ± S.E.: 87.1 % ± 1.1 %), average mapping depth (33.3 ± 0.6 ×), and genome coverage with mapping depth higher than 4 × (95.1 % ± 0.2 %) (Table S1). We identified a total of 3097,336 SNPs, of which 260,756 SNPs were in the exons of functional genes (Table S2), and the nucleotide diversity (π) was 2.44×10^{-3}.

3.2. Demographic history

The results of PSMC showed a declining trend in N_e beginning at *c*. 200 kyr ago (Fig. S1). Using SMC++ based on three different
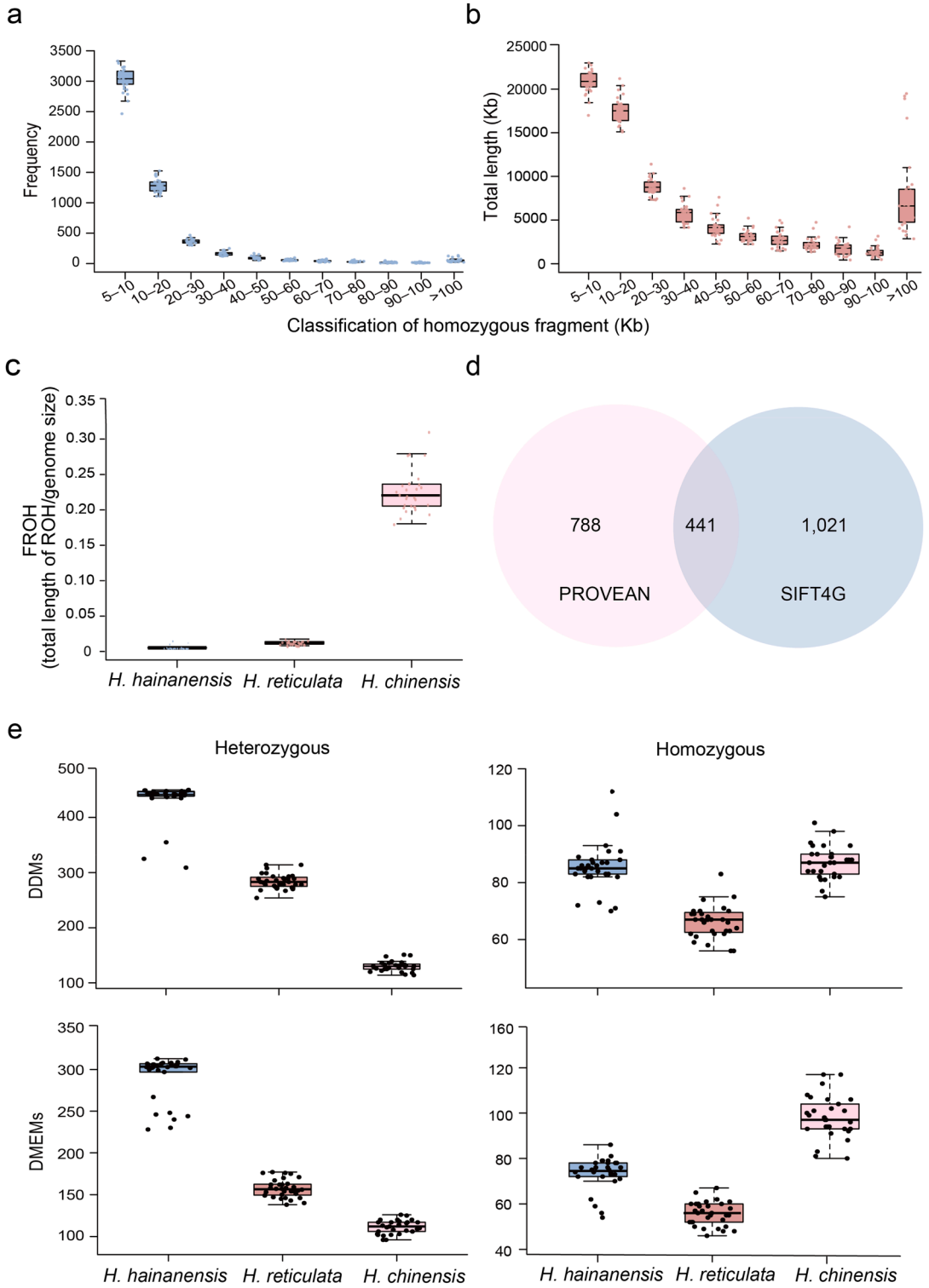
(caption on next page)

Fig. 2. Frequency distribution and total lengths of runs of homozygosity (ROH) in *H. chinensis* with comparisons in the total length of ROH/genome size (FROH) among three *Hopea* species (a-c) and evaluations of genetic loads in *H. chinensis* with comparisons among three *Hopea* species (d, e). **(a-c)**, All indices are calculated for each sampled *H. chinensis* tree (N = 29). **(d)**, The Venn diagram of derived deleterious mutations (DDMs) using the results from PROVEAN and SIFT4G. **(e)**, The accumulation of heterozygous and homozygous DDMs and the derived major-effect mutations (DMEMs) in the genome of each sampled tree. Data of *H. hainanensis* (N = 30) and *H. reticulata* (N = 32) are obtained from Wang et al. (2024). In each boxplot, the center lines, box edges, and whiskers represent medians, the 25 % and 75 % quartiles, and the upper and lower distribution of 1.5 times the quartile range, respectively.

generation times, we found that N_e reached the maximum at *c.* 4500 – 23000 years ago, followed by continuous sharp declines started from about 2900 – 16000 years ago (Fig. 1b). These declines occurred after the LGM and N_e decreased from the maximum (*c.* 1.0 — 5.0 × 10^6) to less than 1000 (Fig. 1b). These results showed similar demographic history to that in *H. hainanensis* and *H. reticulata* (Fig. 1b).

3.3. Genetic consequences of small population size

To explore the consequences of small remnant population size, we estimated both the inbreeding level and the genetic loads. The ROH (runs of homozygosity) analysis showed a high frequency of short homozygous fragments (5 – 20 Kb) in all sampled trees (Fig. 2a). We found only a few homozygous fragments longer than 100 Kb, but the total length of these fragments reached up to 7816 Kb, accounting for 2.3 % of the reference genome size (Fig. 2b). The ROH fragments composed 22.5 % of the *H. chinensis* genome, which was far higher than the other two *Hopea* species (Fig. 2c), indicating high levels of inbreeding.

We identified 441 DDMs (in 425 genes) supported by both analyses using PROVEAN and SIFT4G (Fig. 2d). We found 337 DMEMs in 332 genes (see Methods). Among these deleterious mutations, 278 DDMs (271 genes) and 262 DMEMs (257 genes) were homozygous in at least one sampled tree, with a low number of homozygous deleterious mutations per sampled tree (87.1 ± 1.1 DDMs and 98.1 ± 1.7 DMEMs) being homozygous per sampled tree (Fig. 2e). The genes containing DDMs and DMEMs were not significantly enriched in any pathways (Table S3). Compared to *H. hainanensis* (678 DDMs and 416DMEMs) and *H. reticulata* (617 DDMs and 304 DMEMs), we detected fewer DDMs and DMEMs in *H. chinensis*, but a similar number of DDMs and more DMEMs were observed with homozygotes per sampled tree in this species (Fig. 2e).

3.4. Positively selected genes associated with adaptation

To identify the genes relevant to adaptations of *H. chinensis* at the northern boundary of Dipterocarpoideae, we first investigated the genetic structure within our samples. The analysis using ADMIXTURE showed the lowest cross-validation at *K* = 1 (Fig. 3a), and the first two axes of principal component analysis and the neighbor-joining phylogenomic tree did not show consistent results of genetic clustering (Fig. 3b and c). Thus, all sampled trees belonged to only one genetic group.

Subsequently, we performed selective sweep analysis using three statistics (π, CLR, and Tajima's *D*) to screen the genes with signals of positive selection. We found 4142, 2102, and 8993 positively selected genes, with 49 genes supported by all three statistics (Fig. 3d and e; Table S4). Among these 49 genes, we found five genes (*YUCCA*, small subunit ribosomal protein S8e (*rps8*), laccase (*LAC*), cyclic nucleotide gated channel (*CNGC*), and MYB proto-oncogene protein (*MYB*)) participating in abiotic stress regulation and antioxidation that are relevant to cold and drought tolerance (Table S4). Moreover, we also detected seven positively selected genes involved in biotic stress signaling, plant defense modulating, pathogen response, and nonhost resistance, which are linked with plant defense and immunity (Table S4). In addition, the *MYB*, *LAC*, and *CNGC* were also found to take part in secondary metabolism modulation and pathogen resistance in plant defense and immunity (Table S4).
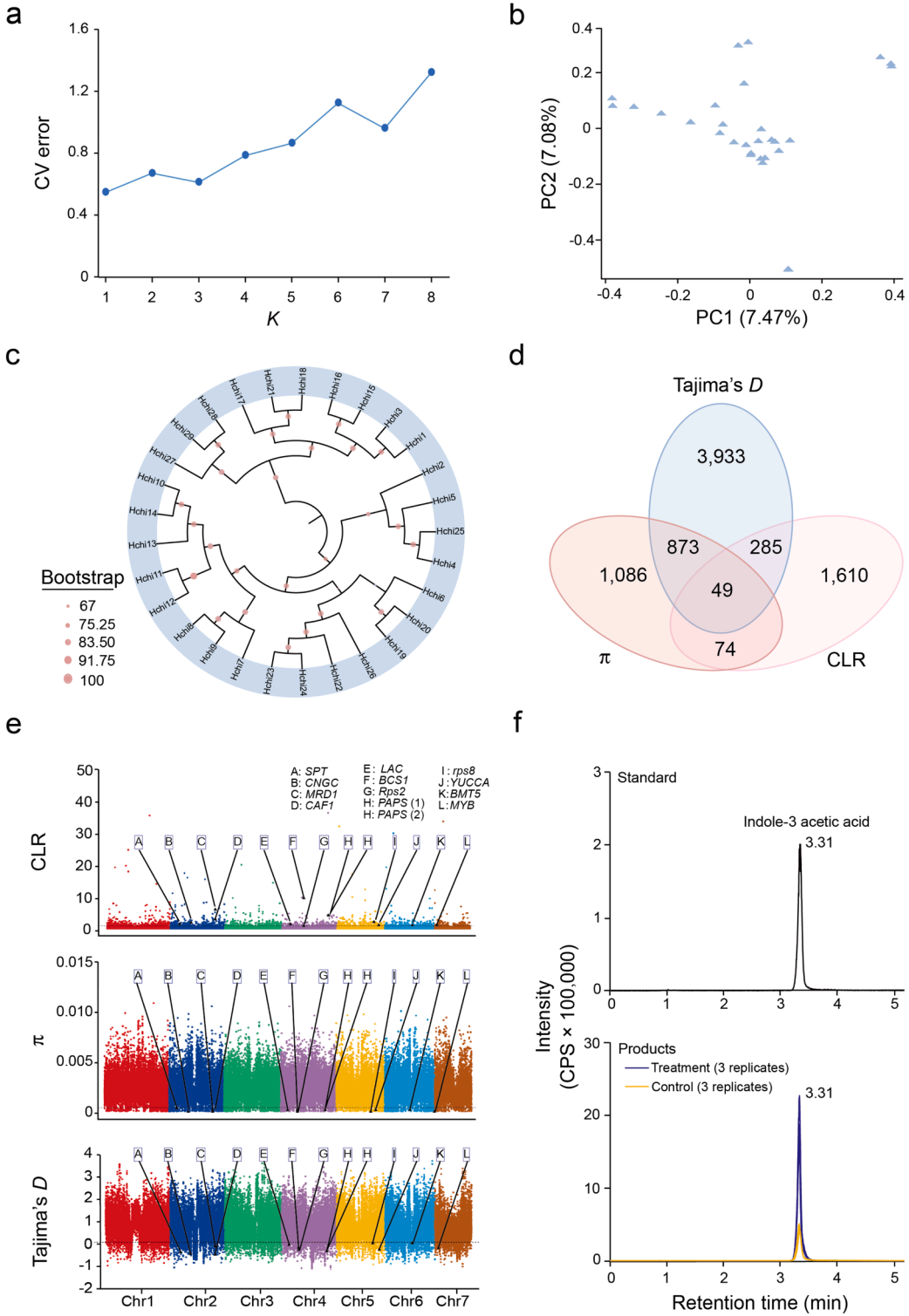
To validate the annotated function of the *YUCCA* gene, we conducted *in vitro* reactions and identified IAA in the products using a UPLC, and the concentration of IAA (represented by the ion intensity) in the *in vitro* reactions was far higher than that in the control reactions (Fig. 3f), confirming the function of this gene.

To further explore the molecular footprints associated with the adaptation of *H. chinensis*, our comparative genomics identified 935 positively selected genes (Fig. 4a; Fig. S2b). Though KEGG enrichment analysis yielded no significant results (Table S5), we found one positively selected gene (25S rRNA (uracil2634-N3)-methyltransferase (*BMT5*)) also supported by all three statistics in the selective sweep analysis (Figs. 3e and 4b; Table S4).

3.5. Expanded and contracted gene families

Our comparative genomics revealed 227 expanded and 52 contracted gene families (Fig. 4a). The expanded gene families were significantly enriched into 18 KEGG pathways, including one and four pathways associated with responses to stresses (anthocyanin biosynthesis (map00942)) and plant defense and immunity (e.g., phenylpropanoid biosynthesis (map00940)) (Table S6). The contracted gene families were significantly enriched into four KEGG pathways participating in carbohydrate metabolism, steroid biosynthesis, and endocytosis (Table S6). Intriguing, we found that 125 specific gene families, among which 23, 22, and 27, are associated with responses to cold and drought and plant defense and immunity (Fig. 4c; Table S7). There were 30 lost gene families in the *H. chinensis* genome, thirteen of which are relevant to abiotic and biotic stresses (Table S8).

a

b

c

Bootstrap
· 67
· 75.25
· 83.50
· 91.75
· 100

d

Tajima's *D*
3,933
873   285
1,086   49   1,610
74
π   CLR

e

A: *SPT*   E: *LAC*   I: *rps8*
B: *CNGC*   F: *BCS1*   J: *YUCCA*
C: *MRD1*   G: *Rps2*   K: *BMT5*
D: *CAF1*   H: *PAPS* (1)   L: *MYB*
           H: *PAPS* (2)

f

Standard

Indole-3 acetic acid
3.31

Products
Treatment (3 replicates)
Control (3 replicates)
3.31

Fig. 3. Genetic structure of sampled *H. chinensis* trees (a-c), results of selective sweep analyses (d, e), and *in vitro* functional assay of indole-3-pyruvate monooxygenase (YUCCA) (f). **(a-c)**, Results of cross-validation error (CV error) of each assumed genetic group number (*K*) show that the optimal *K* value is 1 in genetic clustering analysis, and assignment of sampled trees was also performed according to the first two principal components from the principal component analysis and the neighbor-joining phylogenetic tree (both analyses also show the presence of only one genetic cluster). **(d)**, The Venn diagram of positively selected genes was revealed by three selective sweep analyses (Table S4). **(e)**, Manhattan plots show the distribution of CLR, π, and Tajima's *D* values in each chromosome. We marked the genes supported by all three analyses and associated with the plant's responses to biotic and abiotic environments (Table S4). **(f)**, The standard of indole-3-acetic acid (IAA) (at the concentration of 100 ng/ml) and reaction products (treatment (with enzyme) and control (without enzyme) experiments) are identified using a UPLC.

4. Discussion

Unraveling the genomic characteristics linked with adaptations and population dynamics of species living on the edge of an ecosystem improves our understanding of distributional constraints and future range shifts in the face of environmental changes (Liu et al., 2024; Wang et al., 2023). In this study, our population genomic analysis revealed drastic population declines of *H. chinensis* after the LGM, suggesting the contribution of post-glacial human activities to its endangered status. Though we found high levels of inbreeding in this species, there were only a few DDMs and DMEMs, which were not significantly enriched into any KEGG pathway. Furthermore, selective sweep analysis and comparative genomics detected many genes/gene families associated with responses to biotic and abiotic stresses. These findings infer the factors causing the endangered status, evaluate the genetic consequences of endangerment, and elucidate the adaptive molecular footprints.

All three studied dipterocarp species had similar demographic histories, showing the presence of dramatic post-LGM population declines. These results coincide with the historical records of long-term human activities (Lipson et al., 2018). As many dipterocarp species produce high-quality timbers (Luo et al., 2024), *H. chinensis* may have suffered long-term logging for building architectures and furniture-making. Moreover, our demographic evidence, along with the observation of ongoing severe logging and land use change (Luo et al., 2024; Stibig et al., 2014), further support the dominant role of human disturbances in forming the endangered status of Dipterocarpoideae.

Nevertheless, the recovery of protected species is underpinned by genetic factors (Li et al., 2005). As *H. chinensis* is a diploid species, a small remnant population size is expected to rapidly elevate inbreeding (Bortoluzzi et al., 2020). This is in accordance with our results. Fortunately, unlike other endangered trees (Ma et al., 2021; Yang et al., 2018), the high level of inbreeding has not yet caused a severe accumulation of derived deleterious mutations and major-effect mutations. This is probably because the bottleneck only occurred a few hundred generations ago, and/or strong purifying selection has excluded mutations with serious negative effects on survival and reproduction (Mathur and DeWoody, 2021). Compared with the two congeneric species, we found a similar number of DDMs and more DMEMs that were homozygous in at least one tree, indicating a higher possibility of fixation of a DDM/DMEM in *H. chinensis*, which is likely to lead to negative effects on fitness and consequently cause significant genetic load in the future. Although *H. hainanensis* and *H. reticulata* are autotetraploid species and homozygotes are less likely to be formed than closely related diploid species (Husband et al., 2008; Parisod et al., 2010), our findings show evidence for a certain degree of genetic load in *H. chinensis*.

Genes with signals of positive selection and expanded/contracted gene families form the molecular basis of adaptations (Ma et al., 2024). In this study, many positively selected genes and specific gene families relevant to the responses to cold and drought stresses. These findings coincide with the climate in our sampling area, where the minimum recorded temperature can reach to 0 ℃ and the annual precipitation is only 1200 – 1500 mm (Tan et al., 2005). Thus, these genes/gene families are likely to reflect the consequences of adaptive evolution and assist *H. chinensis* living at the northern boundary of dipterocarps' range. Moreover, we also detected many positively selected genes and specific gene families linked with plant defense and immunity. Given that the composition of herbivores and pathogens may vary drastically across different areas due to changes in climate and environment (Hamann et al., 2021; Makiola et al., 2022), these genes/gene families revealed a potential gene pool specialized for fighting against the endemic natural enemies, which may have been long coevolved with *H. chinensis*. Many lost gene families are also associated with plants' responses to abiotic and biotic stresses. They may be the footprints of long-term evolution driven by the specific climates and natural enemies at the northern boundary of Dipterocarpoideae because the expansion and contraction of gene families generally reflect the needs of organisms in the adaptation to specific environments (Ma et al., 2024). In addition, the gene (*BMT5*) supported by both selective sweep analysis and comparative genomics is likely to contribute to the adaptation to abiotic stresses because it participates in antioxidation and can help *Candida glycerinogenes* tolerate acetic acid stress (Zhou et al., 2024).

Together with our previous findings in other dipterocarp species, we summarized the following conservation strategies for endangered dipterocarps. First, the most urgent conservation intervention is to establish nature reserves completely covering the remaining populations to prevent further anthropogenic interference. Second, to prevent further accumulation of deleterious mutations, it is necessary to mitigate the high levels of inbreeding. Thus, we should carry out conservation efforts to protect pollinators and seed dispersers associated with dipterocarps for ensuring outcrossing (Wang et al., 2020). However, the composition of these organisms and the strength of their interactions with dipterocarps are poorly known, though some tiny insects have been recorded to be pollinators (Kato et al., 2008; Lu et al., 2020). More detailed and quantitative studies on the pollination and seed dispersal networks will be extremely helpful for determining the essential mutualists for endangered dipterocarps. Third, when choosing the locations for *ex-situ* conservation, we ought to pay attention to local abiotic and biotic conditions (Tang et al., 2020). We, therefore, need a comprehensive description of both environmental factors and antagonist assemblages in the native ranges of endangered dipterocarp species and the candidate locations for *ex-situ* conservation to assess the feasibility of transplants. As genomic signatures linked with plant defense and immunity have also been detected in other dipterocarps (Wang et al., 2024), each species may face distinct
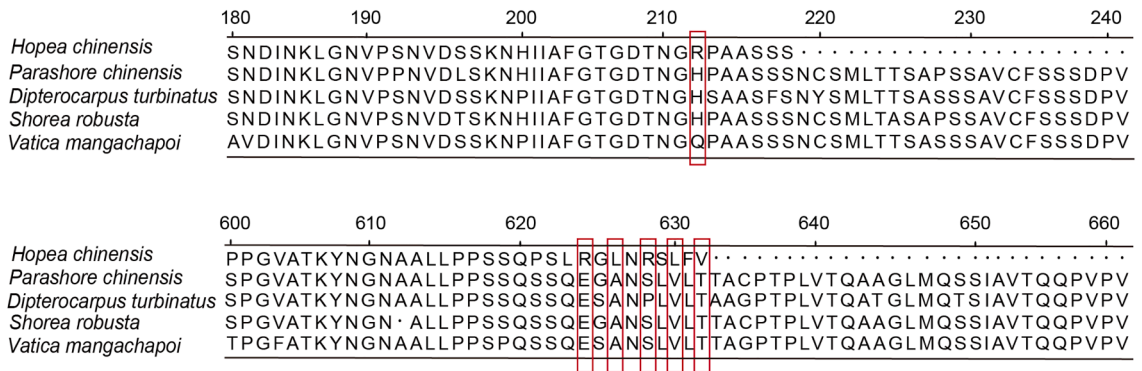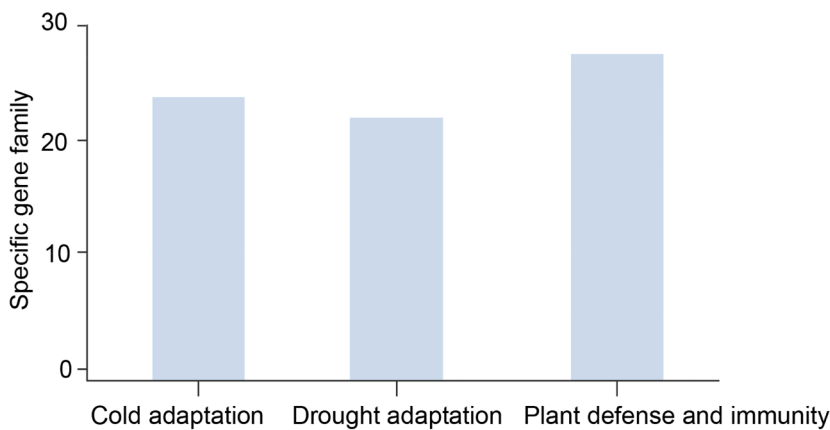
a

Positive selection / Expansion /Contraction
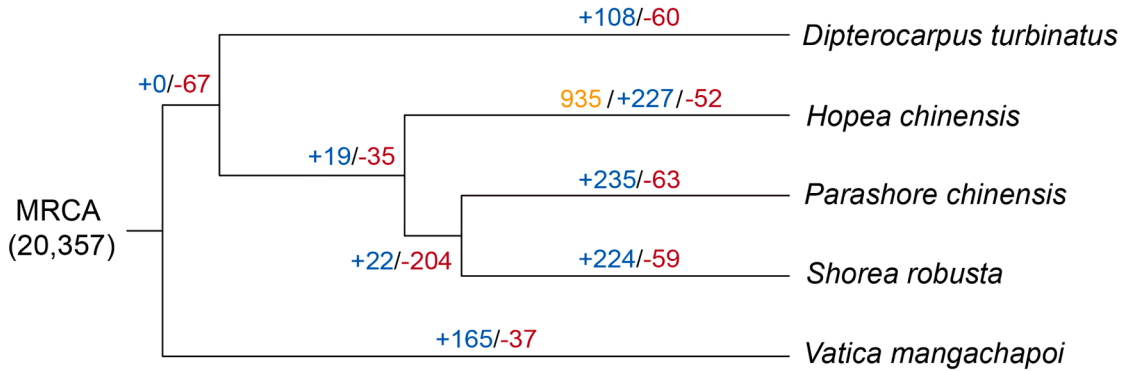
b

BMT5

c

Fig. 4. Comparative genomics between *H. chinensis* and four other dipterocarp species (a), positively selected amino acid sites in the 25S rRNA (uracil2634-N3)-methyltransferase gene (*BMT5*) (b), and the number of specific gene families relevant to cold and drought tolerance and plant defense and immunity (c). **(a)**, The number of positively selected genes and significantly expanded/contracted gene families are shown by orange, blue, and red, respectively. MRCA: the most recent common ancestor. **(b)**, The amino acid sites experiencing positive selection are highlighted by red frames, and the signal of positive selection in these genes is supported by all three selective sweep analyses and comparative genomics. **(c)**, Details of specific gene families are provided in Table S7.

combinations of biotic stresses.

In this study, we reveal the genomic characteristics linked with adaptations to the northern limit of Dipterocarpoideae and potential causative factors explaining the endangered status, providing novel insights into conserving these world's charismatic trees. We highlight the importance of further accumulating genomic studies to reach more comprehensive and representative results for developing more robust actions for Dipterocarpoideae protection. It is also necessary to carry out empirical experiments (e.g., common garden experiments) to examine the associations between genetic variations and adaptations revealed by genomic studies to improve *ex-situ* conservation strategies. As recent human activities have dramatically altered interspecific interactions that have long coevolved and consequently threaten the persistence of species (Wang et al., 2020; Yang et al., 2023), we emphasize the necessity to implement biological conservation beyond the target species by including both mutualistic and antagonistic networks. For policy making and conservation strategy designing, we appeal for establishing nature reserves for endangered dipterocarp species, where human activities should be strictly restricted rather than only protecting wild trees of target species.

Ethics statement

Not applicable: This manuscript does not include human or animal research.

Declaration of Competing Interest

On behalf of the Authors I confirm that there is no conflict of interest in case of the manuscript. Moreover, the authors have declared that no competing interests exist.

Acknowledgments

Appendix A. Supporting information

Supplementary data associated with this article can be found in the online version at doi:10.1016/j.gecco.2024.e03354.

Data Availability

Data will be made available on request.

References

Alexander, D.H., Novembre, J., Lange, K., 2009. Fast model-based estimation of ancestry in unrelated individuals. Genome Res. 19, 1655–1664. https://doi.org/10.1101/gr.094052.109.

Ashton, P., Kettle, C.J., 2012. Dipterocarp biology as a window to the understanding of tropical forest structure: Where are we looking now? Biotropica 44, 575–576. https://doi.org/10.1111/j.1744-7429.2012.00913.x.

Ashton, P.S., Morley, R.J., Heckenhauer, J., Prasad, V., 2021. The magnificent dipterocarps: Précis for an Epitaph? Kew Bull. 76, 87–125. https://doi.org/10.1007/s12225-021-09934-7.

Bansal, M., Morley, R.J., Nagaraju, S.K., Dutta, S., Mishra, A.K., Selveraj, J., Kumar, S., Niyolia, D., Harish, S.M., Abdelrahim, O.B., Hasan, Se, Ramesh, B.R., Dayanandan, S., Morley, H.P., Ashton, P.S., Prasad, V., 2022. Southeast Asian dipterocarp origin and diversification driven by Africa-India floristic interchange. Science 375, 455–460. https://doi.org/10.1126/science.abk2177.

Barstow, M. 2021. Hopea chinensis. The IUCN Red List of Threatened Species 2021: e.T208945147A2815951. https://dx.doi.org/10.2305/IUCN.UK.2021-3.RLTS.T208945147A2815951.en.

Bortoluzzi, C., Bosse, M., Derks, M.F.L., Crooijmans, R.P.M.A., Groenen, M.A.M., Megens, H.-J., 2020. The type of bottleneck matters: Insights into the deleterious variation landscape of small managed populations. Evol. Appl. 13, 330–341. https://doi.org/10.1111/eva.12872.

Chen, S., Zhou, Y., Chen, Y., Gu, J., 2018. fastp: an ultra-fast all-in-one FASTQ preprocessor. Bioinformatics 34, i884–i890. https://doi.org/10.1093/bioinformatics/bty560.

Choi, Y., Sims, G.E., Murphy, S., Miller, J.R., Chan, A.P., 2012. Predicting the functional effect of amino acid substitutions and Indels. PLoS One 7, e46688. https://doi.org/10.1371/journal.pone.0046688.

De Bie, T., Cristianini, N., Demuth, J.P., Hahn, M.W., 2006. CAFE: a computational tool for the study of gene family evolution. Bioinformatics 22, 1269–1271. https://doi.org/10.1093/bioinformatics/btl097.

Ghazoul, J., 2016. Dipterocarp Biology, Ecology, and Conservation. Oxford University Press, Oxford.

Gould, B., Moeller, D.A., Eckhart, V.M., Tiffin, P., Fabio, E., Geber, M.A., 2014. Local adaptation and range boundary formation in response to complex environmental gradients across the geographical range of *Clarkia xantiana* ssp. *xantiana*. J. Ecol. 102, 95–107. https://doi.org/10.1111/1365-2745.12188.

Hamann, E., Blevins, C., Franks, S.J., Jameel, M.I., Anderson, J.T., 2021. Climate change alters plant–herbivore interactions. N. Phytol. 229, 1894–1910. https://doi.org/10.1111/nph.17036.

Huang, S., Chen, H., Tang, W., Luo, W., Wang, Y., 2008. Biological and ecological characteristics of *Hopea chinensis*, a plant endemic to Guangxi. Biodivers. Sci. 16, 15–23. https://doi.org/10.3724/SP.J.1003.2008.07145.

Husband, Brian C., Ozimec, B., Martin, Sara L., Pollock, L., 2008. Mating consequences of polyploid evolution in flowering plants: Current trends and insights from synthetic polyploids. Int J. Plant Sci. 169, 195–206. https://doi.org/10.1086/523367.

Jin, X., Yin, X., Xu, Y., 2015. Effects of light intensity and soil moisture on seed germination of 3 species of Dipterocarpaceae. J. West China For. Sci. 44, 36–40. https://doi.org/10.16473/j.cnki.xblykx1972.2015.01.002.

Kanehisa, M., Goto, S., 2000. KEGG: Kyoto encyclopedia of genes and genomes. Nucleic Acids Res. 28, 27–30. https://doi.org/10.1093/nar/28.1.27.

Kato, M., Kosaka, Y., Kawakita, A., Okuyama, Y., Kobayashi, C., Phimminith, T., Thongphan, D., 2008. Plant–pollinator interactions in tropical monsoon forests in Southeast Asia. Am. J. Bot. 95, 1375–1394. https://doi.org/10.3732/ajb.0800114.

Li, H., Durbin, R., 2009. Fast and accurate short read alignment with Burrows–Wheeler transform. Bioinformatics 25, 1754–1760. https://doi.org/10.1093/bioinformatics/btp324.

Li, H., Durbin, R., 2011. Inference of human population history from individual whole-genome sequences. Nature 475, 493–496. https://doi.org/10.1038/nature10231.

Li, H., Handsaker, B., Wysoker, A., Fennell, T., Ruan, J., Homer, N., Marth, G., Abecasis, G., Durbin, R., Subgroup, G.P.D.P., 2009. The sequence alignment/map format and SAMtools. Bioinformatics 25, 2078–2079. https://doi.org/10.1093/bioinformatics/btp352.

Li, L., Stoeckert Jr., C.J., Roos, D.S., 2003. OrthoMCL: identification of ortholog groups for eukaryotic genomes. Genome Res. 13, 2178–2189. https://doi.org/10.1101/gr.1224503.

Li, W., Ali, I., Han, X., Ullah, S., Yang, M., 2023. Soil C, N, P, K and enzymes stoichiometry of an endangered tree species, *Parashorea chinensis* of different stand ages unveiled soil nutrient limitation factors. Forests 14, 624. https://doi.org/10.3390/f14030624.

Li, Y., Chen, X., Zhang, X., Wu, T., Lu, H., Cai, Y., 2005. Genetic differences between wild and artificial populations of *Metasequoia glyptostroboides*: implications for species recovery. Conserv. Biol. 19, 224–231. https://doi.org/10.1111/j.1523-1739.2005.00025.x.

Li, Y., Liu, Y., Gong, J., Fan, S., Shen, G., Zhou, Y., Fang, Q., Tang, Q., Yang, Y., Wang, R., Chen, X., 2021. Unraveling the roles of various ecological factors in seedling recruitment to facilitate plant regeneration. Ecol. Manag. 492, 119219. https://doi.org/10.1016/j.foreco.2021.119219.

Lipson, M., Cheronet, O., Mallick, S., Rohland, N., Oxenham, M., Pietrusewsky, M., Pryce, T.O., Willis, A., Matsumura, H., Buckley, H., Domett, K., Nguyen, G.H., Trinh, H.H., Kyaw, A.A., Win, T.T., Pradier, B., Broomandkhoshbacht, N., Candilio, F., Changmai, P., Fernandes, D., Ferry, M., Gamarra, B., Harney, E., Kampuansai, J., Kutanan, W., Michel, M., Novak, M., Oppenheimer, J., Sirak, K., Stewardson, K., Zhang, Z., Flegontov, P., Pinhasi, R., Reich, D., 2018. Ancient genomes document multiple waves of migration in Southeast Asian prehistory. Science 361, 92–95. https://doi.org/10.1126/science.aat3188.

Liu, X., Zhang, W., Zhang, Y., Yang, J., Zeng, P., Tian, Z., Sun, W., Cai, J., 2024. Chromosome-scale genomes of *Quercus sichourensis* and *Quercus rex* provide insights into the evolution and adaptation of Fagaceae. J. Genet. Genom. 51, 554–565. https://doi.org/10.1016/j.jgg.2024.03.012.

Lu, Q., Zhua, X., Liu, C., Hu, X., Tang, W., Huang, S., 2020. Pollination biology of *Hopea chinensis*. Guihaia 40, 1628–1637. https://doi.org/10.11931/guihaia.gxzw201903030.

Luo, L., Ye, P., Lin, Q., Liu, M., Hao, G., Wei, T., Sahu, S.K., 2024. From sequences to sustainability: exploring dipterocarp genomes for oleoresin production, timber quality, and conservation. Plant Sci. 346, 112139. https://doi.org/10.1016/j.plantsci.2024.112139.

Ma, H., Liu, Y., Liu, D., Sun, W., Liu, X., Wan, Y., Zhang, X., Zhang, R., Yun, Q., Wang, J., Li, Z., Ma, Y., 2021. Chromosome-level genome assembly and population genetic analysis of a critically endangered rhododendron provide insights into its conservation. Plant J. 107, 1533–1545. https://doi.org/10.1111/tpj.15399.

Ma, X., Vanneste, S., Chang, J., Ambrosino, L., Barry, K., Bayer, T., Bobrov, A.A., Boston, L., Campbell, J.E., Chen, H., 2024. Seagrass genomes reveal ancient polyploidy and adaptations to the marine environment. Nat. Plants 10, 240–255. https://doi.org/10.1038/s41477-023-01608-5.

Makiola, A., Holdaway, R.J., Wood, J.R., Orwin, K.H., Glare, T.R., Dickie, I.A., 2022. Environmental and plant community drivers of plant pathogen composition and richness. N. Phytol. 233, 496–504. https://doi.org/10.1111/nph.17797.

Mathur, S., DeWoody, J.A., 2021. Genetic load has potential in large populations but is realized in small inbred populations. Evol. Appl. 14, 1540–1557. https://doi.org/10.1111/eva.13216.

McKenna, A., Hanna, M., Banks, E., Sivachenko, A., Cibulskis, K., Kernytsky, A., Garimella, K., Altshuler, D., Gabriel, S., Daly, M., DePristo, M.A., 2010. The genome analysis toolkit: a MapReduce framework for analyzing next-generation DNA sequencing data. Genome Res 20, 1297–1303. https://doi.org/10.1101/gr.107524.110.

Myers, N., Mittermeier, R.A., Mittermeier, C.G., da Fonseca, G.A.B., Kent, J., 2000. Biodiversity hotspots for conservation priorities. Nature 403, 853–858. https://doi.org/10.1038/35002501.

Ng, P.C., Henikoff, S., 2003. SIFT: Predicting amino acid changes that affect protein function. Nucleic Acids Res. 31, 3812–3814. https://doi.org/10.1093/nar/gkg509.

Parisod, C., Holderegger, R., Brochmann, C., 2010. Evolutionary consequences of autopolyploidy. N. Phytol. 186, 5–17. https://doi.org/10.1111/j.1469-8137.2009.03142.x.

Pavlidis, P., Živković, D., Stamatakis, A., Alachiotis, N., 2013. SweeD: likelihood-based detection of selective sweeps in thousands of genomes. Mol. Biol. Evol. 30, 2224–2234. https://doi.org/10.1093/molbev/mst112.

Primananda, E., Sunardi, Fefirenta, A.D., Rahmawati, K., Mira, F.R., Budi, S.W., Robiansyah, I., 2023. Survey for threatened plants in riparian fragmented forests: A case study on three *Vatica* (Dipterocarpaceae) species in Kapuas Hulu, West Kalimantan. J. Nat. Conserv. 72, 126367. https://doi.org/10.1016/j.jnc.2023.126367.

Purcell, S., Neale, B., Todd-Brown, K., Thomas, L., Ferreira, M.A.R., Bender, D., Maller, J., Sklar, P., de Bakker, P.I.W., Daly, M.J., Sham, P.C., 2007. PLINK: A tool set for whole-genome association and population-based linkage analyses. Am. J. Hum. Genet. 81, 559–575. https://doi.org/10.1086/519795.

Raes, N., Cannon, C.H., Hijmans, R.J., Piessens, T., Saw, L.G., van Welzen, P.C., Slik, J.W.F., 2014. Historical distribution of Sundaland's dipterocarp rainforests at Quaternary glacial maxima. Proc. Natl. Acad. Sci. USA 111, 16790–16795. https://doi.org/10.1073/pnas.1403053111.

Stibig, H.J., Achard, F., Carboni, S., Raši, R., Miettinen, J., 2014. Change in tropical forest cover of Southeast Asia from 1990 to 2010. Biogeosciences 11, 247–258. https://doi.org/10.5194/bg-11-247-2014.

Tajima, F., 1989. Statistical method for testing the neutral mutation hypothesis by DNA polymorphism. Genetics 123, 585–595. https://doi.org/10.1093/genetics/123.3.585.

Takahashi, Y., Suyama, Y., Matsuki, Y., Funayama, R., Nakayama, K., Kawata, M., 2016. Lack of genetic variation prevents adaptation at the geographic range margin in a damselfly. Mol. Ecol. 25, 4450–4460. https://doi.org/10.1111/mec.13782.

Tan, W., Li, D., Wen, Y., Zhao, Z., 2005. Biodiversity and Conservation System of Guangxi Shiwandashan Nature Reserve. China Environmental Science Press, Beijing.

Tang, R., Li, Y., Xu, Y., Schinnerl, J., Sun, W., Chen, G., 2020. *In-situ* and *ex situ* pollination biology of the four threatened plant species and the significance for conservation. Biodivers. Conserv. 29, 381–391. https://doi.org/10.1007/s10531-019-01887-5.

Tang, W., Mao, S., Pan, b, Huang, S., Mo, L., Luo, W., 2009. Spatial distribution pattern of seed rain and seed gemination characteristics of endangered plant *Hopea chinensis*. J. For. Environ. 29, 149–154. https://doi.org/10.3969/j.issn.1001-389X.2009.02.011.

Tang, W., Dai, W., Hu, X., Huang, S., 2018. ISSR-based genetic diversity of wild and *ex situ* conserved population of *Hopea chinensis* (Merr.) Hand.-Mazz. Bangladesh J. Bot. 44, 407–413. https://doi.org/10.3329/bjb.v44i3.38547.

Terhorst, J., Kamm, J.A., Song, Y.S., 2017. Robust and scalable inference of population history from hundreds of unphased whole genomes. Nat. Genet. 49, 303–309. https://doi.org/10.1038/ng.3748.

Trang, N.T.P., Triest, L., 2016. Genetic structure of the threatened *Hopea chinensis* in the Quang Ninh Province, Vietnam. gmr.15028103 Genet. Mol. Res. 15. https://doi.org/10.4238/gmr.15028103.

Vilella, A.J., Severin, J., Ureta-Vidal, A., Heng, L., Durbin, R., Birney, E., 2009. EnsemblCompara GeneTrees: Complete, duplication-aware phylogenetic trees in vertebrates. Genome Res. 19, 327–335. https://doi.org/10.1101/gr.073585.107.

Wang, K., Li, M., Hakonarson, H., 2010. ANNOVAR: Functional annotation of genetic variants from high-throughput sequencing data. Nucleic Acids Res. 38, e164. https://doi.org/10.1093/nar/gkq603.

Wang, R., Zhang, X., Shi, Y., Li, Y., Wu, J., He, F., Chen, X., 2020. Habitat fragmentation changes top-down and bottom-up controls of food webs. Ecology 101, e03062. https://doi.org/10.1002/ecy.3062.

Wang, R., Liu, C., Segar, S.T., Jiang, Y., Zhang, K., Jiang, K., Wang, G., Cai, J., Chen, L., Chen, S., Cheng, J., Compton, S.G., Deng, J., Ding, Y., Du, F.K., Hu, X., Hu, X., Kang, L., Li, D., Lu, L., Li, Y., Tang, L., Tong, X., Wang, Z., Xu, W., Yang, Y., Zang, R., Zu, Z., Zhang, Y., Chen, X., 2024. Dipterocarpoidae genomics reveal their demography and adaptations to Asian rainforests. Nat. Commun. 15, 1683. https://doi.org/10.1038/s41467-024-45836-5.

Wang, S., Liang, H., Wang, H., Li, L., Xu, Y., Liu, Y., Liu, M., Wei, J., Ma, T., Le, C., Yang, J., He, C., Liu, J., Zhao, J., Zhao, Y., Lisby, M., Sahu, S.K., Liu, H., 2022. The chromosome-scale genomes of *Dipterocarpus turbinatus* and *Hopea hainanensis* (Dipterocarpaceae) provide insights into fragrant oleoresin biosynthesis and hardwood formation. Plant Biotechnol. J. 20, 538–553. https://doi.org/10.1111/pbi.13735.

Wang, T., Meng, H., Wang, N., Zheng, S., Jiang, Y., Lin, D., Song, Y., Kozlowski, G., 2023. Adaptive divergence and genetic vulnerability of relict species under climate change: a case study of *Pterocarya macroptera*. Ann. Bot. 132, 241–254. https://doi.org/10.1093/aob/mcad083.

Wilcove, D.S., Giam, X., Edwards, D.P., Fisher, B., Koh, L.P., 2013. Navjot's nightmare revisited: logging, agriculture, and biodiversity in Southeast Asia. Trends Ecol. Evol. 28, 531–540. https://doi.org/10.1016/j.tree.2013.04.005.

Williamson, S.H., Hubisz, M.J., Clark, A.G., Payseur, B.A., Bustamante, C.D., Nielsen, R., 2007. Localizing recent adaptive evolution in the human genome. PLoS Genet. 3, e90. https://doi.org/10.1371/journal.pgen.0030090.

Wurster, C.M., Bird, M.I., Bull, I.D., Creed, F., Bryant, C., Dungait, J.A.J., Paz, V., Cerling, T.E., 2010. Forest contraction in north equatorial Southeast Asia during the Last Glacial Period. Proc. Natl. Acad. Sci. USA 107, 15508–15511. https://doi.org/10.1073/pnas.1005507107.

Yamamoto, Y., Kamiya, N., Morinaka, Y., Matsuoka, M., Sazuka, T., 2007. Auxin biosynthesis by the *YUCCA* genes in rice. Plant Physiol. 143, 1362–1371. https://doi.org/10.1104/pp.106.091561.

Yang, J., Lee, S.H., Goddard, M.E., Visscher, P.M., 2011. GCTA: a tool for genome-wide complex trait analysis. Am. J. Hum. Genet. 88, 76–82. https://doi.org/10.1016/j.ajhg.2010.11.011.

Yang, Y., Ma, T., Wang, Z., Lu, Z., Li, Y., Fu, C., Chen, X., Zhao, M., Olson, M.S., Liu, J., 2018. Genomic effects of population collapse in a critically endangered ironwood tree *Ostrya rehderiana*. Nat. Commun. 9, 5449. https://doi.org/10.1038/s41467-018-07913-4.

Yang, Y., Zhang, Y., Zhang, Y., Chen, S., Li, Q., Wang, R., Chen, X., 2023. Selection to attract pollinators and to confuse antagonists specializes fig–pollinator chemical communications. J. Syst. Evol. 61, 454–464. https://doi.org/10.1111/jse.12908.

Yang, Z., 2007. PAML 4: Phylogenetic analysis by maximum likelihood. Mol. Biol. Evol. 24, 1586–1591. https://doi.org/10.1093/molbev/msm088.

Zhou, L., Lu, X., Zong, H., Zhuge, B., 2024. Effect of *Candida glycerinogenes* 25S rRNA methyltransferase BMT5 on the stress tolerance of acetic acid and its application. Food Ferment. Ind. 50 (6), 1. https://doi.org/10.13995/j.cnki.11-1802/ts.035295.